Scientia Horticulturae 273 (2020) 109615

Contents lists available at ScienceDirect

Scientia Horticulturae

journal homepage: www.elsevier.com/locate/scihorti

Exploring UAV-imagery to support genotype selection in olive breeding programs

Pilar Rallo[a,*], Ana I. de Castro[b,1], Francisca López-Granados[b], Ana Morales-Sillero[a], Jorge Torres-Sánchez[b], María Rocío Jiménez[a], Francisco M. Jiménez-Brenes[b], Laura Casanova[a], María Paz Suárez[a]

[a] Departamento de Ciencias Agroforestales, ETSIA, Universidad de Sevilla, 41013 Sevilla, Spain
[b] imaPing Group, Department of Crop Protection, Institute for Sustainable Agriculture (IAS), Spanish National Research Council (CSIC), Spain

ARTICLE INFO

Keywords:
Olea europaea L.
Olive breeding
Phenotyping
Plant architecture
Precision agriculture
Unmanned aerial vehicles
OBIA

ABSTRACT

Airborne methodologies based on unmanned aerial vehicles (UAV) are becoming an extraordinary tool for implementing fast, accurate and affordable phenotyping strategies within plant breeding programs. The aim of this paper was to study the potential use of a previously developed UAV-OBIA platform, to fasten and support decision making for olive breeders regarding the selection of the most promising genotypes in terms of tree geometric traits. In particular, we have studied the feasibility of the system to efficiently classify and select olive genotypes according to four architectural parameters: tree height, crown diameter, projected crown area and canopy volume. These vegetative growth traits and their evolution during the first months after planting are key selection criteria in olive breeding programs. On-ground measurements and UAV estimations were recorded over two years (when trees were 15 and 27 months old, respectively) in two olive breeding trials using different training systems, namely intensive open vase and super high-density hedgerows. More than 1000 young trees belonging to 39 olive accessions, including new cross-bred genotypes and traditional cultivars, were assessed. Even though the accuracy in the UAV estimation compared to the on-ground measurements largely improved the second year, both methodologies detected in both years a high variability and significant differences among the studied genotypes, allowing for statistical comparisons among them. Genotype rankings based on the on-ground measures and UAV estimations were compared. The resulting Spearman's rank coefficient correlations were very high, at above 0.85 in most cases, which highlights that very similar genotype classifications were achieved from either field-measured or airborne-estimated data. Thus, UAV imagery may be used to assess geometric traits and to develop rankings for the efficient screening and selection of genotypes in olive breeding programs.

1. Introduction

Since the domestication of the olive (*Olea europaea* L.) approximately 6000 years ago (Diez et al., 2015), olive trees have been grown in the Mediterranean basin where they are the most important fruit crop at present: around 10 million ha in the area, 94 % of the world olive surface (FAOSTAT, http://fao.org). Up to the middle of the twentieth century, olives were grown under rainfed conditions in long-lasting orchards with low investments, empirical technologies and high labor demand, leading to erratic and low yields. Since then, a continuous trend towards the intensification and technification of more productive and mechanized olive plantations, irrigation, pruning and harvesting mechanization, and new growing systems (e.g., super-high-density hedgerows) has taken place (Rallo et al., 2018b) to respond to an increasing demand for olive products, namely olive oil and table olives. In fact, the expansion of olive growing worldwide is a response to the rising interest and increase in the consumption of these products for their high nutritional value and their beneficial effects on human health (Rallo et al., 2018c).

The need for new olive cultivars that are better adapted to these new growing systems and to near-future scenarios (climate change and new abiotic and biotic stresses including new sanitary threats) encourages the development of olive breeding programs in many olive-producing countries, including Israel (Lavee, 1990), Italy (Bellini et al., 2002), Spain (Rallo et al., 2018a, 2008); Tunisia (Dabbou et al., 2012), Turkey (Ozdemir et al., 2013) and Iran (Zeinanloo et al., 2009).

* Corresponding author.
E-mail address: prallo@us.es (P. Rallo).
[1] Present address: Department of Graphic Engineering and Geomatics, University of Cordoba, Campus de Rabanales, Ctra. IV, km. 396, E-14071 Córdoba, Spain.

https://doi.org/10.1016/j.scienta.2020.109615
Received 21 February 2020; Received in revised form 20 July 2020; Accepted 22 July 2020

Nevertheless, the number of new olive cultivars released so far is still scarce compared to other fruit species (Rallo et al., 2018b). The extraordinary length of the juvenile period of this species has constrained the efficiency of olive breeding programs. In addition, cross-breeding olives requires multiple years of intense screening and the thorough field evaluation of a large number of genotypes during the different stages of the breeding process: initial evaluation of seedlings, intermediate evaluation of preselected genotypes, and final evaluation of advanced selections in comparative trials (Rallo et al., 2018b). Plant phenotyping is commonly laborious since many of the traits of interest to breeders require manual assessment in the field, of sometimes complex-to-achieve characteristics, which are frequently prone to human error and subjectivity (Makanza et al., 2018). In the case of woody species such as the olive, phenotyping is even more complex and laborious due to the usually large size of the trees and their irregular geometry, which hampers the assessment of certain traits, such as canopy architectural features. Trees also require more extensive field trials that are costly for breeders to monitor and evaluate. The evaluation of architectural traits and vegetative growth habits in olive breeding is of major importance for estimating the adaptation of new genotypes to mechanization and different growing systems, particularly super-high-density orchards (Rallo et al., 2013; Rosati et al., 2013). Initial vigor traits have also been related to the rapid passing of the juvenile period in olive progenies (De la Rosa et al., 2006; Rallo et al., 2008), and thus, they are commonly assessed and used as selection criteria in breeding programs (Hammami et al., 2011).

The development of accurate and automatic airborne methodologies based on unmanned aerial vehicles (UAV) represents an extraordinary and powerful tool for phenotyping plant species. In fact, their potential use to extract phenotypic data from large breeding populations to accelerate the selection of new and improved cultivars is currently being investigated over a wide range of species and target traits. For instance, UAV platforms have been used to select high yielding genotypes in cotton (Jung et al., 2018); for the ranking of wheat, barley, and triticale accessions for their potential bioethanol production (Ostos-Garrido et al., 2019); the screening of wild tomatoes for salt tolerance (Johansen et al., 2019); the evaluation of maize genotype performance under low-N conditions (Buchaillot et al., 2019); dry bean responses to abiotic stresses (Sankaran et al., 2018); or the screening of inbred lettuce lines for their carotenoid contents (Maciel et al., 2019).

The use of different sensor technologies to acquire field data on olives and other woody crops (e.g., vineyards, citrus, almonds, and poplars) in experimental trials or commercial groves has also been explored. Most of these studies have been focused on agronomic applications to improve field management, such as weed mapping (Jimenez-Brenes et al., 2019), disease detection (Calderon et al., 2013; De Castro et al., 2015), site-specific phytosanitary sprays (de Castro et al., 2018a), biomass estimation (Peña et al., 2018), irrigation (Caruso et al., 2019; de Castro et al., 2018b), pruning impact quantification (Jimenez-Brenes et al., 2017) or the evaluation of tree damage caused by straddle harvesters (Perez-Ruiz et al., 2018). Other airborne imagery applications in olive include real-time tree counting (Salami et al., 2019), the identification of field-grown cultivars (Avola et al., 2019) and the estimation of plant architectural features (Moriondo et al., 2016; Noori and Panda, 2016). However, information regarding the application of UAV platforms for olive breeding purposes is almost nonexistent. To the best of our knowledge, there is only one previous study that has explored the possible use of UAV imagery in olive breeding trials to estimate the plant height and crown diameter (Diaz-Varela et al., 2015). Nevertheless, specific data on its application to the screening and selection of the best performing genotypes has not been reported.

Recently, our research team developed and validated a high-throughput UAV-based system to estimate multitemporal architectural traits accurately in very young olive trees during breeding trials (De Castro et al., 2019). That system consisted of UAV flight configurations in terms of the flight altitude and image overlaps and an automatic and accurate object-based image analysis (OBIA) algorithm based on photogrammetric point clouds. The present study aimed at exploring the reliability of the former methodology to support decision making in olive breeding programs regarding the selection of the most promising genotypes on the basis of UAV estimated architectural traits. In particular, data from the previously developed workflow (De Castro et al., 2019) were tested at the genotype level to verify the potential use to correctly sort and select 39 olive genotypes grown in two olive breeding trials at two timepoints: 15 and 27 months after planting. Particular attention has been given to the comparison of genotype rankings based on each methodology.

2. Materials and methods

2.1. Field trials and plant material

This experiment was performed in two olive trials belonging to the University of Sevilla (US) table olive breeding program located in Morón de la Frontera, Sevilla (37.193 °N, 5.476 °W, WGS84). The plant material evaluated in the trials included breeding selections and traditional table olive cultivars from different Mediterranean countries (Tables 1 and 2), some of which have been used as progenitors in the US breeding program. The breeding selections are cross-bred genotypes that were previously selected after 3–5 years of initial evaluation in the field for optimal fruit traits (size, pulp-to-pit ratio, and low bruising incidence, among others). The selected original seedlings of these genotypes were clonally propagated by rooting softwood cuttings under mist to produce sufficient number of plants per genotype for the study trials. The trees were planted in the field in October 2015, when both trials were established.

Each trial employed a different training system, namely intensive open vase trees (intensive trial) and super high-density hedgerows (hedgerow trial) (Fig. 1). The intensive trial comprised 25 olive genotypes (12 traditional cultivars and 13 breeding selections, Table 1) with 10 trees per genotype arranged in a randomized design, with two trees

Table 1
Genotypes evaluated in the intensive open vase system trial. The country of origin of traditional cultivars and the progenitors of the genotypes selected within the University of Sevilla (US) olive breeding program are shown.

Genotype names	Origin
Traditional Cultivars	
'Aggezi Shami'	Egypt
'Ascolana Tenera'	Italy
'Hojiblanca'	Spain
'Imperial'	Spain
'Kalamon'	Greece
'Manzanilla Cacereña'	Spain
'Manzanilla de Sevilla'	Spain
'Memecik'	Turkey
'Picholine Marrocaine'	Morocco
'Toffahi'	Egypt
'Uovo di Piccione'	Italy
'Belluti'	Turkey
US Breeding Selections	
05-389	'Manzanilla de Sevilla' x 'Santa Caterina'
06-194	'Manzanilla de Sevilla' x 'Hojiblanca'
06-1158	'Ascolana Tenera' open pollination
06-1176	'Ascolana Tenera' open pollination
06-1308	'Belluti' open pollination
06-1388	'Toffahi' open pollination
06-1439	'Toffahi' open pollination
06-1476	'Toffahi' open pollination
06-1510	'Toffahi' open pollination
06-1577	'Toffahi' open pollination
06-1590	'Toffahi' open pollination
07-038	'Ascolana Tenera' x 'Uovo di Piccione'
07-083	'Ascolana Tenera' x 'Uovo di Piccione'

Table 2
Genotypes evaluated in the super high-density hedgerow system trial. The country of origin of traditional cultivars and the progenitors of the genotypes selected within the University of Sevilla (US) olive breeding program.

Genotype names	Origin
Traditional Cultivars	
'Ascolana Tenera'	Italy
'Hojiblanca'	Spain
'Manzanilla Cacereña'	Spain
'Manzanilla de Sevilla'	Spain
'Memecik'	Turkey
'Toffahi'	Egypt
US Breeding Selections	
06-999	'Ascolana Tenera' open pollination
06-1158	'Ascolana Tenera' open pollination
06-1173	'Ascolana Tenera' open pollination
07-078	'Ascolana Tenera' x 'Uovo di Piccione'
07-192	'Gordal Sevillana' open pollination
07-214	'Gordal Sevillana' open pollination
08-463	'Toffahi' open pollination
08-507	'Toffahi' open pollination

per elementary plot and five repetitions (Fig. 1 A left side and B). The trees were planted in a 7 × 5 m layout and were trained as a single-trunk open vase intended for mechanical harvesting by trunk shaker. In the hedgerow trial, 14 different genotypes (six traditional cultivars and eight breeding selections, Table 2) were included (Fig. 1A right side and C). The experimental design consisted of continuous rows of 20 trees per genotype (elementary plot) with three randomly arranged repetitions. The trees were planted in a 5 × 1.75 m layout and were trained to a central leader to form a continuous hedgerow to allow for mechanical harvesting by straddle harvester. Both trials were planted following a North-South orientation, and they were drip-irrigated and had guard rows.

2.2. Phenotyping at the ground level: field measurements

The major architectural traits were manually assessed at each field trial in January 2017 and January 2018 (15 and 27 months after planting), coinciding with the dates of the UAV flights. The maximum tree heights were measured for all individual trees with a telescopic ruler in both the intensive (244 trees) and hedgerow (806 trees) trials.

The canopy traits (crown diameter, area and volume) were assessed for all the trees in the intensive trial (244 trees), and, in the case of the hedgerow trial, for four trees per elementary plot (164 trees). The height of the canopy (Hc) and the maximum projected horizontal width (D_1) and its perpendicular (D_2) length were measured with a measuring tape. The mean crown diameter was calculated. The crown area and volume were estimated as in Ben Sadok et al. (2015), assuming an elliptical shape [Π x $((D_1+D_2)/4)^2$] and a cone-shaped form [1/3 x Crown area x Hc], for intensive and hedgerow trees, respectively.

2.3. Phenotyping by using a UAV platform

Data from the application of a previously developed and validated workflow (De Castro et al., 2019) were used. This UAV-based workflow consisted of two primary steps, i) the generation of 3D photogrammetric point clouds and ii) the automatic analysis of the point clouds using an OBIA algorithm to generate and evaluate a set of agronomic traits of great importance in olive phenotyping, such as the tree height, diameter, area and volume of the crown of each tree and of each genotype.

2.3.1. Generation of the 3D point cloud

The generation of the 3D photogrammetric point cloud requires the acquisition of UAV images with high overlaps between them as inputs, and the registration of the coordinates of some ground control points in every field.

The aerial images were acquired in January 2017 and 2018 using a low-cost, commercial, off-the-shelf camera, a Sony ILCE-6000 model

Fig. 1. General aerial and field views of the olive breeding trials in 2018: intensive open vase trial (A left side and B) and super high-density hedgerow trial (A right side and C). (For interpretation of the references to colour in this figure legend, the reader is referred to the web version of this article).

(Sony Corporation, Tokyo, Japan), which was installed on board a quadcopter model MD4-1000 (microdrones GmbH, Siegen, Germany). This camera has a 23.5 × 15.6 mm APS-C CMOS sensor, which is capable of acquiring 24 megapixel (6,000 × 4,000 pixels) images with 8-bit radiometric resolution, and it is equipped with a 20 mm fixed lens. The camera originally captured spectral information in the red, blue and green bands of the electromagnetic spectrum; however, it was modified to capture information in the near infrared (NIR), red, and green bands. The UAV routes were designed to take images from a nadir point of view at a 50 m flight altitude, which resulted in a spatial resolution of 1 cm. The selected forward and side overlaps among the images were 93 % and 60 %, respectively; this configuration has been shown to allow for the accurate 3D modelling of woody crops in previous research (Torres-Sanchez et al., 2015; 2018).

The coordinates of six ground control points from every breeding trial were registered using a real-time kinematic (RTK) GPS linked to a reference station from the GNSS RAP network from the Institute for Statistics and Cartography of Andalusia (IECA), Spain. The estimated accuracy of the GNSS-RTK system is 0.02 m in planimetry and 0.03 m in altimetry.

The images and their coordinates were used as input into Agisoft PhotoScan Professional Edition (Agisoft LLC, St. Petersburg, Russia) version 1.2.4 build 1874, for the generation of the 3D point clouds. The process was fully automatic, with the exception of the manual localization of the ground control points in both olive orchards. The final points in the 3D point clouds were saved in. las format. More information about the processing parameters of this software can be found in Torres-Sanchez et al. (2018) and De Castro et al. (2019).

2.3.2. Automatic analysis of the 3D point clouds

The segmentation and characterization of the olive trees was achieved using the OBIA algorithm reported in De Castro et al. (2019). The work presented here is an extension of a broader research project. Once the rule-set was developed and duly validated, the next step was testing the ability of this approach to phenotype olive genotypes in breeding programs efficiently. Since one of the primary interests of phenotyping studies is to rank different varieties for the target geometric trait, the generated information was used to assess a set of specific variety rankings to select the most promising accessions. This algorithm was created using the Cognition Network programming language in eCognition Developer 9 software (Trimble GeoSpatial, Munich, Germany). The algorithm is fully automatic, and the only inputs needed are the point clouds from every breeding trial and a vector layer with its limits. The algorithm can be divided into the following automatically executed steps: 1. Digital terrain model (DTM) generation (the lower points in the point cloud were selected); 2. Tree point cloud creation (the OBIA algorithm calculated the height of all the points over this reference surface. A new point cloud called *Tree point clouds* containing all the points with heights over 0.30 m was created); 3. Tree crown delineation (a grid was overlaid on the field, and all the squares containing points from the *Tree point clouds* were classified as *Tree*); 4. Point cloud slicing (the *Tree point cloud* was divided into slices. Considering that the field had previously been divided into squares, the point cloud was divided into 3D pixels (*voxels*)); 5. Olive tree characterization (knowing the voxel volume and the number of voxels it was possible to find the volume occupied by the olive crown. Finally, the crown area, length and width were extracted from the classification performed during the second step of the algorithm).

The output of the algorithm is a vector file that includes the crown limits of every tree and contains, as associated information, its crown volume, maximum height, projected area, length and width. This file can be used in any geographic system, and all the information can also be exported as an ASCII file, including the previous information plus the central coordinate of every tree. More details about the OBIA algorithm can be found in De Castro et al. (2019).

2.4. Statistical analysis

The mean values per genotype were calculated for all the field-measured and OBIA-estimated traits. An analysis of variance (ANOVA) of all the measured and estimated traits per genotype were performed, and the mean values were compared using Tukey's test ($p \leq 0.05$). The genotypes were sorted and graphically represented according to every mean field value.

As an estimation of the bias at the genotype level, the relative differences between on-ground-measured and OBIA-estimated data were calculated for each individual tree per genotype using ((field value-OBIA value)/field value)*100. The ANOVA of the relative differences per genotype was also performed and the mean values were compared according to Tukey's test ($p \leq 0.05$). The linear regression fits and correlation coefficients (r) between the measured and estimated plant heights were calculated at the genotype level for each year and training system.

The Spearman's rank correlation coefficients (r_s) between the rankings of genotypes obtained by field data and by OBIA estimations (according to mean values per genotype) were calculated for each trait, year and training system.

All the statistical analyses were performed using Statgraphics Centurion X64.

3. Results

3.1. Genotype characterization and classification

The olive tree identification by UAV-OBIA reached 100 % accuracy. Figs. 2–5 represent the mean values per genotype of all the measured traits in the field, and the same traits were estimated using the UAV-OBIA algorithm for both trials (intensive and hedgerow) and years (2017 and 2018).

High variability and significant differences among the genotypes were observed for all the traits and years using both methodologies (on-ground and OBIA data). The genotypes were sorted in the figures according to the values of the ground-measured traits to detect differences in the relative order graphically, with respect to the OBIA-estimated values.

During the first year of the experiment (2017) (Figs. 2 and 3), the differences between the field and OBIA data were particularly large for the crown area and volume. In the intensive trial (Fig. 2), the relative order of genotypes according to field records differed moderately compared to the OBIA-estimated data classification, although the separation of the genotypes with the lowest values from the genotypes with the highest values was highly conserved between methods. The relative order seemed to be better achieved in the hedgerow trial, and the separation of genotypes with the lowest and highest values was almost the same for the field and OBIA methods (Fig. 3).

One year later, in January 2018, when the trees were 27 months old, there were fewer differences between the field measured and OBIA-estimated traits both in the mean values per genotype and in the relative classification of the genotypes, as observed in the intensive (Fig. 4), and, particularly, in the hedgerow trials (Fig. 5). For example, in the intensive trial, the genotypes with the significantly lowest field tree heights were 06 − 1176, 'Imperial', 05 − 389, 06 − 1590, 'Toffahi', 06 − 1158, 'Belluti' and 'Memecik', and the ones with the significantly largest heights were 06-1476, 'Picholine Marocaine', 'Manzanilla de Sevilla', 06-1308, 06-1439, 'Kalamon', 06-1510, 'Hojiblanca', 'Aggezi Shami' and 'Manzanilla Cacereña'. The same genotypes would be selected for their significantly lower or higher tree height values as estimated by the drone, with just a few exceptions: 06-1476, 'Manzanilla de Sevilla' and 06-1308, which were considered to be within the intermediate tree height group. Furthermore, the mean values within each group were alike for both methods: the shortest trees (approximately 2 m high), and the largest ones (approximately 2.5 m). A similar pattern

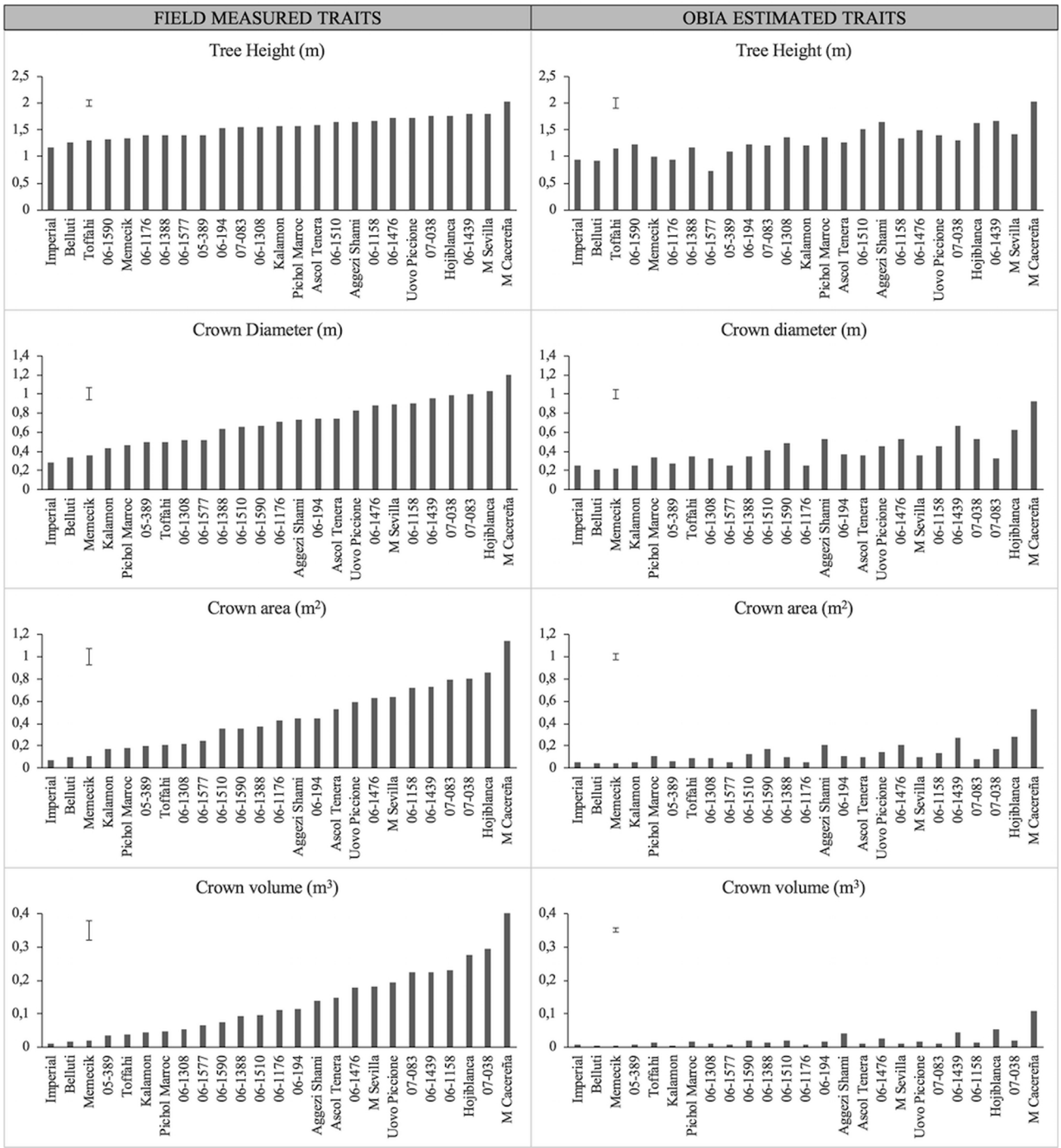

Fig. 2. Intensive open vase system trial January 2017: mean values per genotype of field-measured and OBIA-estimated traits. The genotypes are ordered according to the values measured in the field. The bar represents the mean squared error (MSE).

was observed for the rest of the traits in the same trial and in the hedgerow trial (Fig. 5). That is, two years after planting, the estimation of the trait value and the genotype order (used for further selection within the breeding scheme) via UAV-OBIA was clearly improved.

3.2. UAV estimation accuracy

The mean relative differences between field-measured and OBIA-estimated values per genotype and year for all the traits considered in the study are shown in Table 3 (intensive trial) and Table 4 (hedgerow trial). In the intensive trial (Table 3), the mean relative differences in 2017 (15 months-old trees) were generally high, although they differed among the following traits: plant height (mean 18 %; range 0–51% among genotypes), crown diameter (40 %; 15–68 %), crown area (64 %; 30–90 %) and crown volume (78 %; 41–95 %). The following year, when the trees were approximately 27 months old, the relative differences were notably reduced for the plant height (mean 6%; range 1–17 %) crown diameter (8 %; 2–16 %) and crown area (24 %; 12–36 %), especially the ranges of variation among genotypes. Relative differences for crown volume (68 %; 58–75 %) were still high in 2018, although slightly reduced compared to the previous year. Nevertheless, despite the high mean values and the large ranges of variation among genotypes, the relative differences between both methods (on-ground measures and OBIA estimations) for both years were only significant

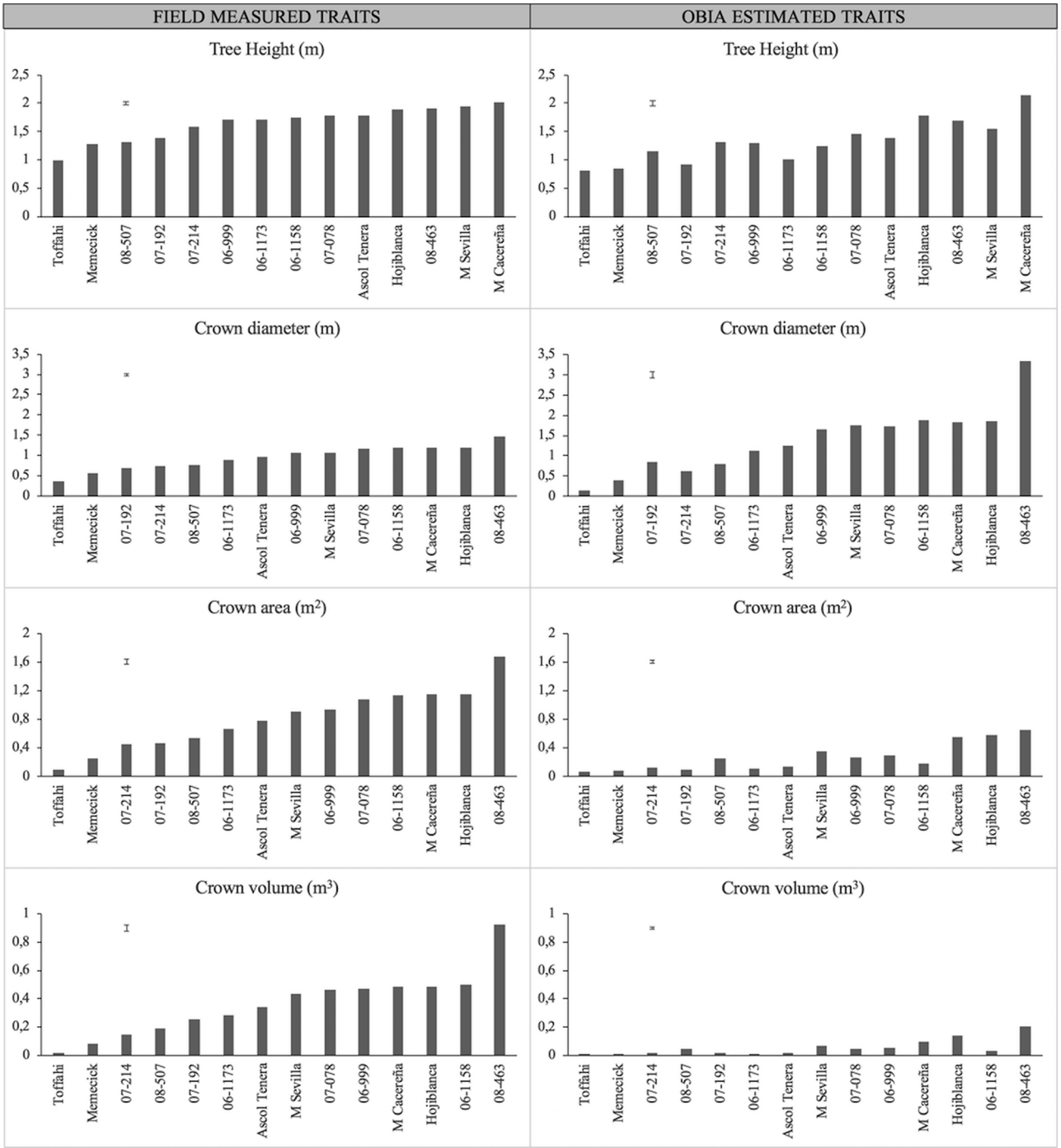

Fig. 3. Super high-density hedgerow system trial January 2017: mean values per genotype of field-measured and OBIA-estimated traits. The genotypes are ordered according to the values measured in the field. The bar represents the mean squared error (MSE).

between the genotypes with the furthest mean values. For example, when measuring the tree height in 2017, the relative differences were only significant between the genotypes with the lowest values (highest accuracy) ('Manzanilla Cacereña, 0 %, and 'Aggezi Shami' 1 %) compared to the genotypes with the highest relative field-OBIA differences (lowest accuracy) (06 − 1176, 30 %, and 06 − 1577, 50 %). The accuracy of the estimated tree height in the remaining 25 genotypes did not differ significantly. Similar conclusions may be obtained for the rest of the traits for both years. The differences were positive in all cases, showing in the intensive trial that the UAV workflow underestimates all the studied traits.

In the hedgerow trial (Table 4), the relative differences in the first year (2017) were similar to those observed in the intensive trial (Table 3), with the exception of the crown diameter: tree height (mean 20 %; range −7 to 38 % among genotypes), crown diameter (44 %; range -128 to 60 %), crown area (65 %; 25–84 %) and crown volume (82 %; 46–95 %). Again, during the second year of the study, the relative differences between field measurements and OBIA estimations were remarkably reduced for the tree height (mean 9 %; range 5–16 % among genotypes), crown diameter (4 %; −8 to 6 %), crown area (10 %; 3–18%) and crown volume (14 %; −14 to 35 %). There was a particularly noticeable reduction in the values of the relative differences in the crown volume (mean 14 %, Table 4) with respect to the intensive trial (mean 68 %, Table 3). As previously shown in the

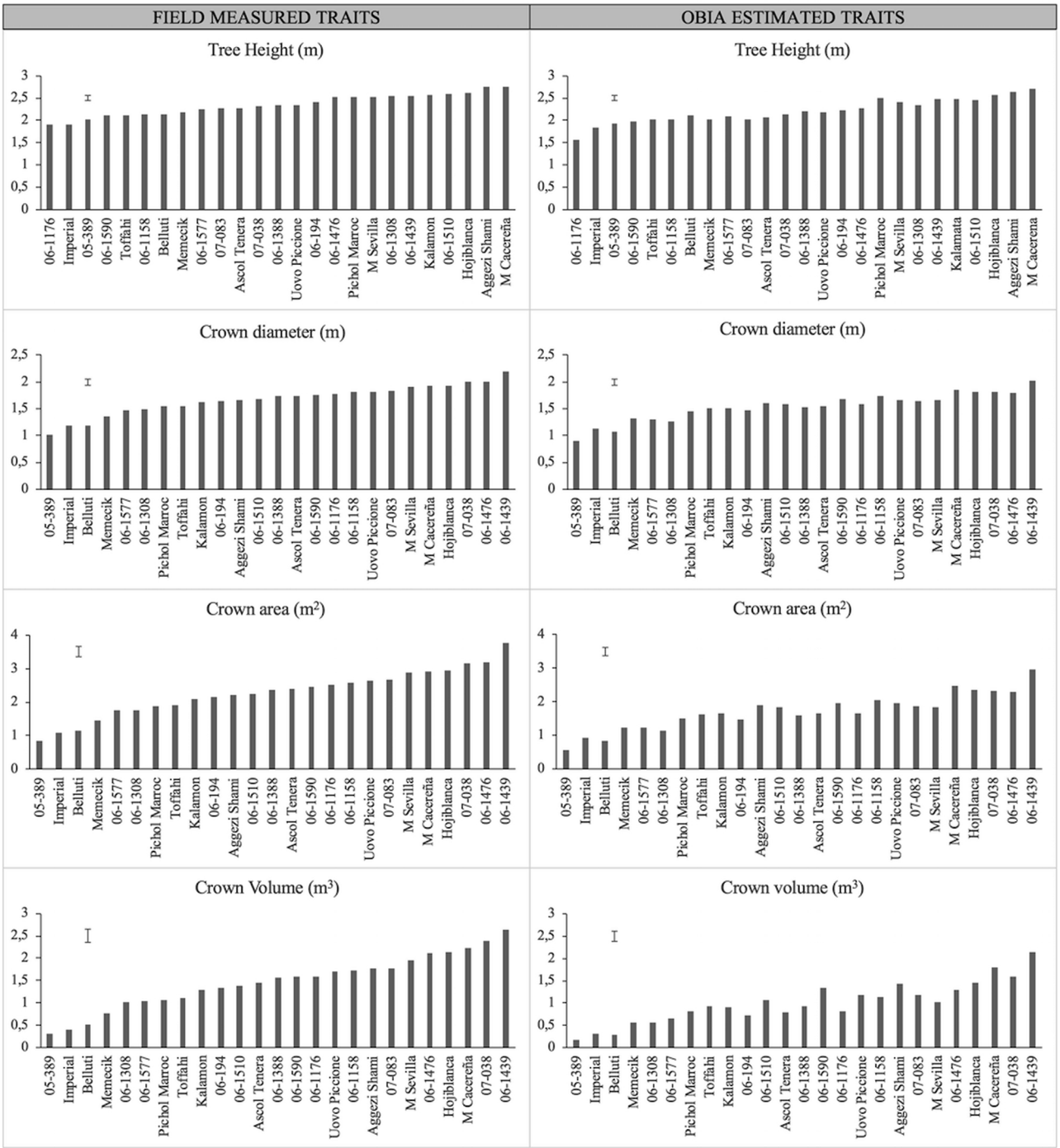

Fig. 4. Intensive open vase system trial January 2018: mean values per genotype of field-measured and OBIA-estimated traits. The genotypes are ordered according to the values measured in the field. The bar represents the mean squared error (MSE).

intensive trial, significant differences in the accuracy of the OBIA estimation were only found between genotypes with the furthest values of the relative differences, and in 2018, no differences at all were found among the genotypes for the crown area and volume, i.e., the same "relative estimation error" was made in every genotype.

The linear fits and correlation coefficients (r) of the measured *vs* the estimated tree heights for each genotype are shown in Fig. 6 (intensive trial) and 7 (hedgerow trial). During the first year of the study, the r values were very different depending on the genotype, ranging between 0.04 (06-1176) and 0.97 (06-1388) in the intensive trial. Lower values were observed in the hedgerow trial, ranging between 0.08 ('Manzanilla Cacereña') and 0.86 (08-507 and 07-192). Nevertheless, for most genotypes, the r was above 0.5 (21 out of 25 in the intensive trial and 9 out of 14 in the hedgerow). Better linear fits were obtained the following year, with correlation coefficients reaching values above 0.75 in all the genotypes of the hedgerow trial (ranging from 0.77 to 0.97, Fig. 7), and above 0.7 in 21 out of 25 genotypes of the intensive trial (range 0.28 − 0.97, Fig. 6)

3.3. Genotype rankings correlations

Spearman's rank correlation coefficients (r_s) (Table 5) measure the statistical dependence between the rankings of genotypes achieved by ordering the mean values according to the field measurements and the

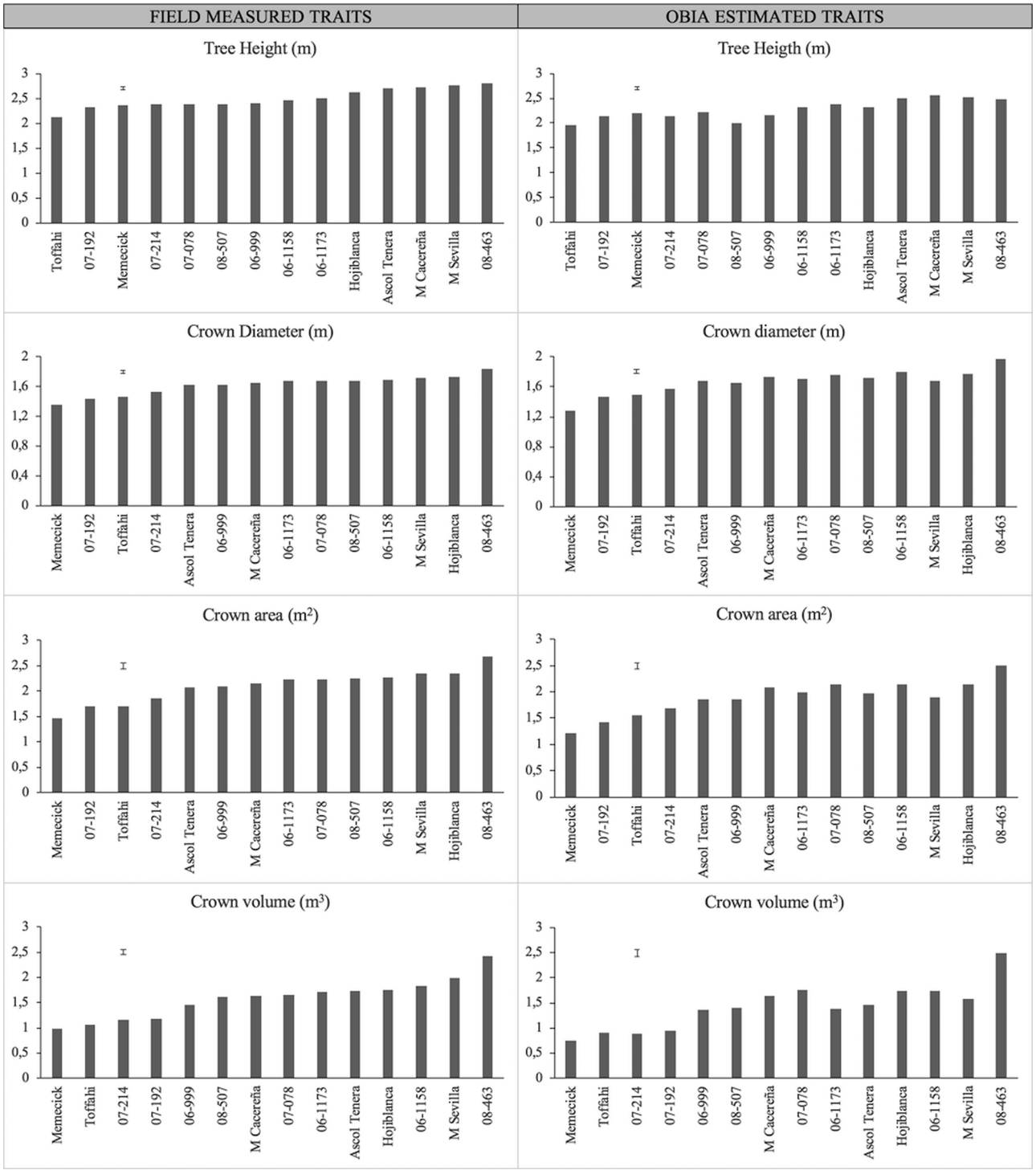

Fig. 5. Super high-density hedgerow system trial trial January 2018: mean values per genotype of field-measured and OBIA-estimated traits. The genotypes are ordered according to the values measured in the field. The bar represents the mean squared error (MSE).

OBIA estimates. In both trials and years, the obtained coefficient values were very high for all the studied traits, although slight differences were found. During the first year of the study, the r_s ranged from 0.69 to 0.87 in the intensive trial, and from 0.79 to 0.97 in the hedgerow trial, showing the lowest values for the crown volume in both trials. The following year, all the coefficients were above 0.91 and 0.85 in the intensive and hedgerow trials, respectively.

4. Discussion

The development of airborne methodologies based on UAV coupled to different sensors offers an extraordinary opportunity for the implementation of fast, accurate and affordable screening strategies in plant breeding programs, and so they are increasingly being used for phenotyping genetic trials on different crops, including some tree species, such as *Pinus halepensis* (Santini et al., 2019); citrus varieties and rootstocks (Ampatzidis and Partel, 2019) and apples (Virlet et al., 2016). Nevertheless, the particular use of UAV platforms for

Table 3
Intensive open vase system trial: mean relative differences (%) between field-measured and OBIA-estimated values for each genotype and year.

GENOTYPE	Tree height		Crown diameter		Crown area		Crown Volume	
	2017	2018	2017	2018	2017	2018	2017	2018
05-389	22 abcd	4 abc	44 abcde	11 abc	68 bcde	31 bcd	77 abc	73 def
06-1158	19 abcd	5 abc	49 bcde	4 ab	77 cde	21 abcd	93 c	68 abcdef
06-1176	30 cd	17 d	62 de	11 abc	82 cde	33 cd	86 bc	74 f
06-1308	13 abc	8 abc	34 abc	16 c	53 abcd	35 d	76 abc	74 ef
06-1388	18 abcd	6 abc	48 abcde	13 abc	74 cde	34 cd	88 bc	74 def
06-1439	7 abc	2 ab	30 ab	7 abc	62 abcde	21 abcd	79 bc	58 a
06-1476	13 abc	10 bcd	39 abcd	10 abc	67 abcde	28 abcd	83 bc	70 bcdef
06-1510	9 abc	6 abc	38 abcd	6 abc	64 abcde	17 abc	82 bc	63 abcde
06-1577	51 d	7 abc	51 abcde	12 abc	75 bcde	29 abcd	90 abc	72 cdef
06-1590	7 abc	7 abc	27 ab	5 ab	51 abcd	20 abcd	69 abc	60 ab
06-194	20 abcd	7 abc	47 bcde	10 abc	70 bcde	29 abcd	74 abc	73 def
07-038	26 bcd	8 abc	46 abcde	9 abc	77cde	26 abcd	93 c	70 bcdef
07-083	22 abcd	11 cd	68 e	11 abc	90 e	30 bcd	95 c	68 abcdef
Aggezi Shami	1 ab	4 abc	29 ab	4 ab	53 abcd	12 a	67 abc	67 abcdef
Ascol Tenera	20 abcd	9 abc	47 bcde	11 abc	71 cde	31 bcd	89 bc	73 def
Belluti	28 bcd	1 ab	35 abcd	11 abc	53 abcd	27 abcd	72 abc	74 def
Hojiblanca	7 abc	1 ab	39 abcd	5 abc	68 bcde	19 abcd	80 bc	67 abcdef
Imperial	21 abcd	3 abc	15 a	4 ab	30 a	15 ab	41 a	60 ab
Kalamon	24 abcd	4 abc	35 abcd	7 abc	53 abcd	21 abcd	72 abc	67 abcdef
M Cacereña	0 a	2 ab	23 ab	3 ab	52 abc	15 ab	74 abc	63 abcd
M Sevilla	21 abcd	6 abc	60 cde	14 bc	85 de	36 d	93 c	75 f
Memecik	26 abcd	7 abc	38 abcd	3 ab	57 abcd	14 ab	73 abc	66 abcdef
Pichol Marroc	14 abc	1 a	25 ab	5 abc	38 ab	19 abcd	62 abc	61 abc
Toffahi	12 abc	5 abc	30 abc	2 a	54 abcde	14 ab	56 ab	60 ab
Uovo Piccione	20 abcd	7 abc	44 abcde	9 abc	71 cde	25 abcd	84 bc	67 abcdef
Mean*	18	6	40	8	64	24	78	68

Different letters indicate significant differences among genotypes for the relative difference according to Tukey ($p \leq 0.05$).
* Absolute values were considered to calculate the mean.

phenotyping olive breeding trials has barely been studied (Diaz-Varela et al., 2015; De Castro et al., 2019).

In the present study, information is given on the feasibility of a high-throughput system based on UAV imagery and a robust point cloud-based OBIA algorithm recently developed by our group (De Castro et al., 2019) to be used as a tool to support olive breeder's decision making. Particularly, we have explored its ability to classify and select the best performing genotypes efficiently according to four architectural traits, namely tree height, crown diameter, projected crown area and canopy volume.

In the first year of the study (2017) (Figs. 2 and 3 and Tables 3 and 4), the UAV estimations differed moderately from the on-ground measurements: the mean relative differences ranged from 18 % for the tree height to 82 % for the crown volume. A general underestimation of tree heights through UAV-based platforms has been reported in other tree species (Kattenborn et al., 2014; Peña et al., 2018), particularly in young plantations. Regarding crown parameters, estimation errors were higher since the small size of the trees during the first year hampered the reconstruction of the canopies. However, it should be stressed that for the calculation of the crown area and volume in the field, geometrical assumptions need to be made, for example, the crown area was assimilated to an ellipse, and the crown volume was likened to a cone. Although these assumptions are widely used (Ben Sadok et al., 2015), they produce inexact field-based estimations compared to the data obtained through airborne imagery that allows for the reconstruction of the entire tree crown (Torres-Sanchez et al., 2015). In fact, similar traits

Table 4
Hedgerow trial: mean relative differences (%) between field-measured and OBIA-estimated values for each genotype and year.

GENOTYPE	Tree height		Crown diameter		Crown area		Crown Volume	
	2017	2018	2017	2018	2017	2018	2017	2018
06-1158	29 def	6 ab	−53 b	−7 a	84 e	3 a	95 c	2 a
06-1173	41 g	5 a	−19 bcd	−2 ab	80 e	10 a	95 c	21 a
06-999	26 def	10 cde	−46 bc	−1 ab	72 bcde	14 a	88 bc	2 a
07-078	18 cd	7 abc	−46 bc	−5 ab	73 cde	3 a	90 bc	−14 a
07-192	38 fg	8 abcde	12 cde	−2 ab	73 bcde	18 a	94 bc	35 a
07-214	18 cd	10 cde	20 de	−3 ab	75 de	9 a	90 bc	22 a
08-463	12 bc	11 de	−128 a	−8 a	61 bcde	3 a	78 bc	−8 a
08-507	12 bc	16 f	13 de	−2 ab	50 abc	14 a	70 b	17 a
Ascol Tenera	22 cde	8 abcd	−22 bcd	−4 ab	84 e	11 a	95 c	17 a
Hojiblanca	5 ab	12 e	−54 b	−3 ab	48 ab	7 a	71 b	0 a
M Cacereña	−7 a	6 ab	−51 bc	−5 ab	51 abcd	3 a	80 bc	−2 a
M Sevilla	20 cd	9 bcde	−62 b	3 ab	63 bcde	18 a	85 bc	21 a
Memecick	34 efg	7 abc	32 de	6 b	72 bcde	17 a	73 bc	25 a
Toffahi	19 cd	8 abcd	60 e	−2 ab	25 a	8 a	46 a	12 a
Mean*	20	9	44	4	65	10	82	14

Different letters indicate significant differences among genotypes for the relative difference according to Tukey ($p \leq 0.05$).
* Absolute values were considered to calculate the mean.

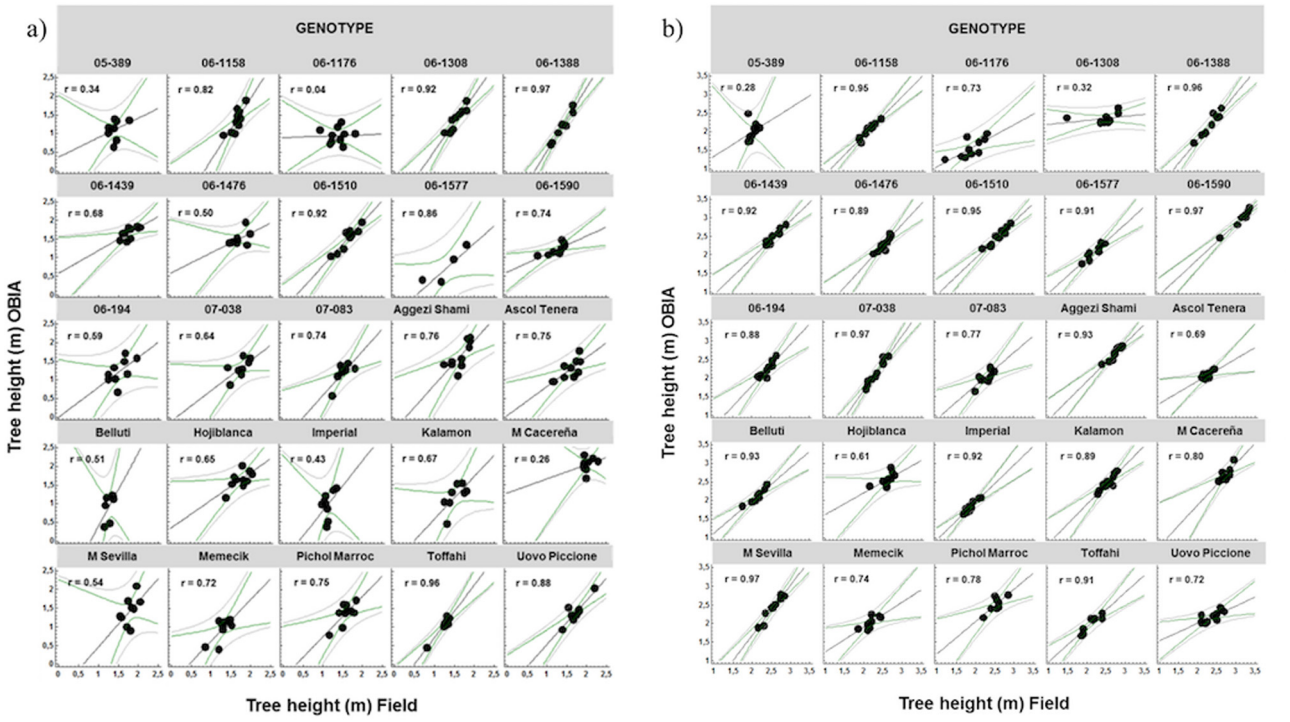

Fig. 6. Tree height correlation between field and OBIA-estimated data for each genotype in the intensive open vase system trial. a) January 2017; b) January 2018.

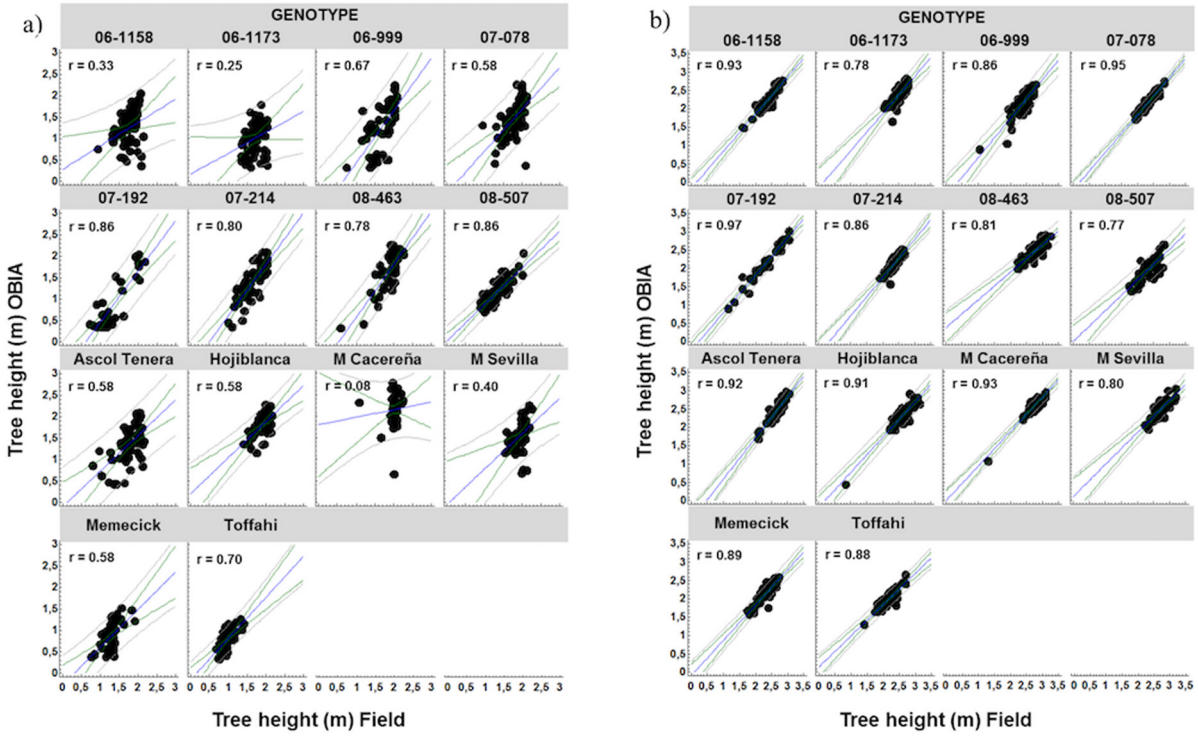

Fig. 7. Tree height correlation between field and OBIA-estimated data for each genotype in the super high-density hedgerow system trial. a) January 2017; b) January 2018.

such as the crown projection area in peach trees (Mu et al., 2018) or the canopy cover in maize field trials (Makanza et al., 2018) were assessed in a more objective manner using UAV platforms, compared to visual assessment.

Besides, when analyzing the results at the genotype level, the above-mentioned differences between the field and OBIA values were only significant among a few individuals for each trait, namely those with the furthest relative errors (Tables 3 and 4). This means that for most

Table 5
Spearman's Rank correlation coefficients (r_s) between the genotype rankings based on field measurements and OBIA estimations for each trait, year and training system.

	Intensive		Hedgerow	
	2017	2018	2017	2018
Tree Height	0.8706	0.9607	0.9165	0.8813
Crown Diameter	0.8013	0.9552	0.9692	0.8681
Crown Area	0.7525	0.9354	0.9033	0.8901
Crown Volume	0.6892	0.9192	0.7890	0.8549

individuals, the relative error in the estimation was similar, and thus, the relative comparison among genotypes would not be affected. This idea is particularly important for phenotyping purposes in breeding programs, i.e., that the value of the trait itself is not as decisive in the selection process as the relative performance of the genotypes for the target trait.

The OBIA estimations largely improved the second year of the study (2018), as evidenced by the notable reduction in the relative differences for all the traits in both trials (Figs. 4 and 5), although it was especially remarkable in the hedgerow trial when estimating crown area and volume (Table 4). In fact, no significant differences were found among the genotypes for the relative error in any of the crown traits studied here. The lower relative differences observed in the crown volume from the hedgerow trial seem to indicate that the cone shape assumption made for the calculation of volume fits better for trees trained to a central leader in the hedgerow trial compared to the open vase trees. The influence of higher plant densities on the canopy volume and vegetative growth traits has been previously reported in olive hedgerow trials (Gomez-del-Campo et al., 2017; Trentacoste et al., 2015).

As mentioned above, the tree height was the best estimated trait during both years and trials, showing the lowest mean relative difference between the field and OBIA data (Tables 3 and 4). For most genotypes, the estimation error was the same, and significant differences were only found between the shortest genotype (06-1176) and the tallest ones ('Manzanilla Cacereña', 'Hojiblanca', 06-1439), which showed significantly lower relative differences (Table 3 and Fig. 4). The loss of accuracy in the height estimation for the shortest trees has been already observed (Torres-Sanchez et al., 2015). The linear regression figures (Figs. 6 and 7) show very good fits for this trait at the genotype level during the second year of the experiment, with correlation coefficients (r) above 0.8 in most cases. Diaz-Varela et al. (2015) reported very similar values regarding the determination coefficient in an olive hedgerow trial ($R^2 = 0.66$) and much lower results ($R^2 = 0.14$) in an open vase trial. By contrast, lower r coefficients were observed in the present study during the previous year, with no linear adjustment ($r < 0.5$), although only in particular genotypes, with five out of 25 in the intensive trial and four out of 14 in the hedgerow.

Finally, Spearman's rank coefficient correlations were used to check if similar genotype rankings could be created from either field-measured or OBIA-estimated data (Table 5). The high values obtained for all the traits and years (above 0.85 in most cases), ranging between 0.69 for the crown volume in the intensive trial the first year of study (2017) and 0.97 in the hedgerow trial for the same year highlights that both methodologies could be used to assess the significant differences among genotypes, leading to very similar rankings, even though errors would be made in the estimation of particular trait values (Tables 3 and 4). Although high accuracy could be desirable in estimating the trait via UAV technology in other types of field trials, regarding breeding goals, it is more important to achieve a good relative classification (ranking) of the plant material in order to select the genotypes with the best performance, rather than the absolute value of the trait itself, as previously mentioned.

5. Conclusions

The present study reports the usefulness of UAV-imagery, an image analysis based on photogrammetric point clouds and an automated OBIA algorithm, previously developed by our group (De Castro et al., 2019), to assess individual genotype performance in detail, and to develop an effective ranking of genotypes that would allow for the selection of the best performing individuals in terms of tree architecture. The results here presented confirm the reliability and robustness of this approach to support olive breeder's decision making. UAV-based monitoring may dramatically reduce the time and cost of evaluating in the field the large number of progenies that are generated in olive breeding programs, thus speeding up the selection process and increasing the overall efficiency of these programs.

Author contributions

PR, MPS and FLG conceived and designed the experiments; PR, MPS, AMS, MRJ and LC, performed the field experiments, collected and processed the ground- based data; AIdC, JTS, FMJB and FLG performed the UAV flights and processed the imagery; PR and MPS analyzed the data; FLG, PR and MPS contributed with equipment and analysis tools; PR wrote the paper; MPS, FLG and AIdC revised the manuscript. All authors have read and approved the manuscript.

Declaration of Competing Interest

The authors declare that they have no known competing financial interests or personal relationships that could have appeared to influence the work reported in this paper.

Acknowledgements

The breeding field trials in which the experiments were performed are funded by Interaceituna (Spanish Inter-Professional Association for Table Olives) through the FIUS projects PR201402347 and PRJ201703174. This research was partly financed by the AGL2017-83325-C4-4-R Project (Spanish Ministry of Science, Innovation and Universities and AEI-EU-FEDER funds), and Intramural-CSIC 201840E002 Projects. Research of A.I. de Castro was supported by the Juan de la Cierva Incorporación Program of the Spanish MINECO funds The authors thank Dr. José Ordovás for his advice and help in statistical analysis, and Aceitunas Guadalquivir S.L. for the maintenance of the field trials.

References

Ampatzidis, Y., Partel, V., 2019. UAV-based high throughput phenotyping in citrus utilizing multispectral imaging and artificial intelligence. Remote Sens. 11 (4), 410. https://doi.org/10.3390/rs11040410.

Avola, G., Di Gennaro, S.F., Cantini, C., Riggi, E., Muratore, F., Tornambe, C., Matese, A., 2019. Remotely sensed vegetation indices to discriminate field-grown olive cultivars. Remote Sens. 11 (10), 1242. https://doi.org/10.3390/rs11101242.

Bellini, E., Giordani, E., Parlati, M.V., Pandolfi, S., 2002. Olive genetic improvement: thirty years of research. Acta Hortic. 586, 105–108. https://doi.org/10.17660/ActaHortic.2002.586.13.

Ben Sadok, I., Martinez, S., Moutier, N., Garcia, G., Leon, L., Belaj, A., De La Rosa, R., Khadari, B., Costes, E., 2015. Plasticity in vegetative growth over contrasted growing sites of an F1 olive tree progeny during its juvenile phase. PLoS One 10 (6), e0127539. https://doi.org/10.1371/journal.pone.0127539.

Buchaillot, M.L., Gracia-Romero, A., Vergara-Diaz, O., Zaman-Allah, M.A., Tarekegne, A., Cairns, J.E., Prasanna, B.M., Araus, J.L., Kefauver, S.C., 2019. Evaluating maize genotype performance under low nitrogen conditions using RGB UAV phenotyping techniques. Sensors 19 (8), 1815. https://doi.org/10.3390/s19081815.

Calderon, R., Navas-Cortes, J.A., Lucena, C., Zarco-Tejada, P.J., 2013. High-resolution airborne hyperspectral and thermal imagery for early, detection of Verticillium wilt of olive using fluorescence, temperature and narrow-band spectral indices. Remote Sens. Environ. 139, 231–245. https://doi.org/10.1016/j.rse.2013.07.031.

Caruso, G., Zarco-Tejada, P.J., Gonzalez-Dugo, V., Moriondo, M., Tozzini, L., Palai, G., Rallo, G., Hornero, A., Primicerio, J., Gucci, R., 2019. High-resolution imagery acquired from an unmanned platform to estimate biophysical and geometrical

parameters of olive trees under different irrigation regimes. PLoS One 14. https://doi.org/10.1371/journal.pone.0210804.
Dabbou, S., Chaieb, I., Rjiba, I., Issaoui, M., Echbili, A., Nakbi, A., Gazzah, N., Hammami, M., 2012. Multivariate data analysis of fatty acid content in the classification of olive oils developed through controlled crossbreeding. J. Am. Oil Chem. Soc. 89, 667–674. https://doi.org/10.1007/s11746-011-1946-1.
De Castro, A.I., Ehsani, R., Ploetz, R., Crane, J.H., Abdulridha, J., 2015. Optimum spectral and geometric parameters for early detection of laurel wilt disease in avocado. Remote Sens. Environ. 171, 33–44. https://doi.org/10.1016/j.rse.2015.09.011.
De Castro, A.I., Jimenez-Brenes, F.M., Torres-Sanchez, J., Peña, J.M., Borra-Serrano, I., Lopez-Granados, F., 2018a. 3-D Characterization of vineyards using a novel UAV imagery-based OBIA procedure for precision viticulture applications. Remote Sens. 10. https://doi.org/10.3390/rs10040584.
De Castro, A.I., Maja, J.M., Owen, J., Robbins, J., Peña, J.M., 2018b. Experimental approach to detect water stress in ornamental plants using sUAS-imagery. In: Conference on Autonomous Air and Ground Sensing Systems for Agricultural Optimization and Phenotyping III. Spie-Int Soc Optical Engineering. Orlando, FL.
De Castro, A.I., Rallo, P., Suárez, M.P., Torres-Sánchez, J., Casanova, L., Jiménez-Brenes, F.M., Morales-Sillero, A., Jiménez, M.R., López-Granados, F., 2019. High-throughput system for the early quantification of major architectural traits in olive breeding trials using UAV images and OBIA techniques. Front. Plant Sci. 10, 1472. https://doi.org/10.3389/fpls.2019.01472.
De la Rosa, R., Kiran, A.I., Barranco, D., Leon, L., 2006. Seedling vigour as a preselection criterion for short juvenile period in olive breeding. Aust. J. Agric. Res. 57, 477–481. https://doi.org/10.1071/AR05219.
Diaz-Varela, R.A., de la Rosa, R., Leon, L., Zarco-Tejada, P.J., 2015. High-resolution airborne UAV imagery to assess olive tree crown parameters using 3D photo reconstruction: application in breeding trials. Remote Sens. 7, 4213–4232. https://doi.org/10.3390/rs70404213.
Diez, C.M., Trujillo, I., Martinez-Urdiroz, N., Barranco, D., Rallo, L., Marfil, P., Gaut, B.S., 2015. Olive domestication and diversification in the Mediterranean Basin. New Phytol. 206, 436–447. https://doi.org/10.1111/nph.13181.
Gomez-del-Campo, M., Connor, D.J., Trentacoste, E.R., 2017. Long-term effect of intra-row spacing on growth and productivity of super-high density hedgerow olive orchards (cv. Arbequina). Front. Plant Sci. 8. https://doi.org/10.3389/fpls.2017.01790.
Hammami, S.B.M., Leon, L., Rapoport, H.F., De la Rosa, R., 2011. Early growth habit and vigour parameters in olive seedlings. Sci. Hortic. 129, 761–768. https://doi.org/10.1016/j.scienta.2011.05.038.
Jimenez-Brenes, F.M., Lopez-Granados, F., de Castro, A.I., Torres-Sanchez, J., Serrano, N., Pena, J.M., 2017. Quantifying pruning impacts on olive tree architecture and annual canopy growth by using UAV-based 3D modelling. Plant Methods 13. https://doi.org/10.1186/s13007-017-0205-3.
Jimenez-Brenes, F.M., Lopez-Granados, F., Torres-Sanchez, J., Peña, J.M., Ramirez, P., Castillejo-Gonzalez, I.L., de Castro, A.I., 2019. Automatic UAV-based detection of Cynodon dactylon for site-specific vineyard management. PLoS One 14. https://doi.org/10.1371/journal.pone.0218132.
Johansen, K., Morton, M.J.L., Malbeteau, Y.M., Aragon, B., Al-Mashharawi, S.K., Ziliani, M.G., Angel, Y., Fiene, G.M., Negrao, S.S.C., Mousa, M.A.A., Tester, M.A., McCabe, M.F., 2019. Unmanned aerial vehicle-based phenotyping using morphometric and spectral analysis can quantify responses of wild tomato plants to salinity stress. Front. Plant Sci. 10. https://doi.org/10.3389/fpls.2019.00370.
Jung, J.H., Maeda, M., Chang, A.J., Landivar, J., Yeom, J., McGinty, J., 2018. Unmanned aerial system assisted framework for the selection of high yielding cotton genotypes. Comput. Electron. Agric. 152, 74–81. https://doi.org/10.1016/j.compag.2018.06.051.
Kattenborn, T., Sperlich, M., Bataua, K., Koch, B., 2014. Automatic single tree detection in plantations using UAV-based photogrammetric point clouds. Int. Arch. Photogramm. Remote Sens. Spatial Inf. Sci. XL-3, 139–144. https://doi.org/10.5194/isprsarchives-XL-3-139-2014.
Lavee, S., 1990. Aims, methods, and advances in breeding of new olive (*Olea europaea* L) cultivars. Acta Hortic. 286, 23–36. https://doi.org/10.17660/ActaHortic.1990.286.1.
Maciel, G.M., Gallis, R.B.D., Barbosa, R.L., Pereira, L.M., Siquieroli, A.C.S., Peixoto, J.V.M., 2019. Image phenotyping of inbred red lettuce lines with genetic diversity regarding carotenoid levels. Int. J. Appl. Earth Obs. Geoinf. 81, 154–160. https://doi.org/10.1016/j.jag.2019.05.016.
Makanza, R., Zaman-Allah, M., Cairns, J.E., Magorokosho, C., Tarekegne, A., Olsen, M., Prasanna, B.M., 2018. High-throughput phenotyping of canopy cover and senescence in maize field trials using aerial digital canopy imaging. Remote Sens. 10. https://doi.org/10.3390/rs10020330.
Moriondo, M., Leolini, L., Stagliano, N., Argenti, G., Trombi, G., Brilli, L., Dibari, C., Leolini, C., Bindi, M., 2016. Use of digital images to disclose canopy architecture in olive tree. Sci. Hortic. 209, 1–13. https://doi.org/10.1016/j.scienta.2016.05.021.
Mu, Y., Fujii, Y., Takata, D., Zheng, B.Y., Noshita, K., Honda, K., Ninomiya, S., Guo, W., 2018. Characterization of peach tree crown by using high-resolution images from an unmanned aerial vehicle. Hortic. Res. 5. https://doi.org/10.1038/s41438-018-0097-z.
Noori, O., Panda, S.S., 2016. Site-specific management of common olive: remote sensing, geospatial, and advanced image processing applications. Comput. Electron. Agric. 127, 680–686. https://doi.org/10.1016/j.compag.2016.07.031.
Ostos-Garrido, F.J., de Castro, A.I., Torres-Sanchez, J., Piston, F., Peña, J.M., 2019. High-throughput phenotyping of bioethanol potential in cereals using UAV-based multi-spectral imagery. Front. Plant Sci. 10. https://doi.org/10.3389/fpls.2019.00948.
Ozdemir, Y., Tangu, N.A., Akcay, M.E., 2013. Generating omega-3 rich olive oil by cross breeding. Eur. J. Lipid Sci. Technol. 115, 977–981. https://doi.org/10.1002/ejlt.201300026.
Peña, J.M., de Castro, A.I., Torres-Sanchez, J., Andujar, D., San Martin, C., Dorado, J., Fernandez-Quintanilla, C., Lopez-Granados, F., 2018. Estimating tree height and biomass of a poplar plantation with image-based UAV technology. Aims Agric. Food 3, 313–326. https://doi.org/10.3934/agrfood.2018.3.313.
Perez-Ruiz, M., Rallo, P., Jimenez, M.R., Garrido-Izard, M., Suarez, M.P., Casanova, L., Valero, C., Martinez-Guanter, J., Morales-Sillero, A., 2018. Evaluation of over-the-row harvester damage in a super-high-density olive orchard using on-board sensing techniques. Sensors 18. https://doi.org/10.3390/s18041242.
Rallo, P., Jimenez, R., Ordovas, J., Suarez, M.P., 2008. Possible early selection of short juvenile period olive plants based on seedling traits. Aust. J. Agric. Res. 59, 933–940. https://doi.org/10.1071/AR08013.
Rallo, L., Barranco, D., Castro-Garcia, S., Connor, D.J., del Campo, M.G., Rallo, P., 2013. High-density olive plantations. In: In: Janick, J. (Ed.), Horticultural Reviews Vol 41. John Wiley & Sons, Chichester, pp. 303–383.
Rallo, L., Barranco, D., De la Rosa, R., Leon, L., 2018a. New olive cultivars and selections in Spain: results after 25 years of breeding. Acta Hortic. 1199, 21–25. https://doi.org/10.17660/ActaHortic.2018.1199.4.
Rallo, L., Barranco, D., Díez, C.M., Rallo, P., Suárez, M.P., Trapero, C., Pliego-Alfaro, F., 2018b. Strategies for olive (Olea europaea L.) breeding: cultivated genetic resources and crossbreeding. al., e. In: Al-Khayri, J.M. (Ed.), Advances in Plant Breeding Strategies: Fruits. Springer International Publishing AG.
Rallo, L., Diez, C.M., Morales-Sillero, A., Miho, H., Priego-Capote, F., Rallo, P., 2018c. Quality of olives: a focus on agricultural preharvest factors. Sci. Hortic. 233, 491–509. https://doi.org/10.1016/j.scienta.2017.12.034.
Rosati, A., Paoletti, A., Caporali, S., Perri, E., 2013. The role of tree architecture in super high-density olive orchards. Sci. Hortic. 161, 24–29. https://doi.org/10.1016/j.scienta.2013.06.044.
Salami, E., Gallardo, A., Skorobogatov, G., Barrado, C., 2019. On-the-fly olive tree counting using a UAS and cloud services. Remote Sens. 11. https://doi.org/10.3390/rs11030316.
Sankaran, S., Zhou, J.F., Khot, L.R., Trapp, J.J., Mndolwa, E., Miklas, P.N., 2018. High-throughput field phenotyping in dry bean using small unmanned aerial vehicle based multispectral imagery. Comput. Electron. Agric. 151, 84–92. https://doi.org/10.1016/j.compag.2018.05.034.
Santini, F., Kefauver, S.C., de Dios, V.R., Araus, J.L., Voltas, J., 2019. Using unmanned aerial vehicle-based multispectral, RGB and thermal imagery for phenotyping of forest genetic trials: a case study in Pinus halepensis. Ann. Appl. Biol. 174, 262–276. https://doi.org/10.1111/aab.12484.
Torres-Sanchez, J., Lopez-Granados, F., Serrano, N., Arquero, O., Peña, J.M., 2015. High-throughput 3-D monitoring of agricultural-tree plantations with unmanned aerial vehicle (UAV) technology. PLoS One 10. https://doi.org/10.1371/journal.pone.0130479.
Torres-Sanchez, J., de Castro, A.I., Peña, J.M., Jimenez-Brenes, F.M., Arquero, O., Lovera, M., Lopez-Granados, F., 2018. Mapping the 3D structure of almond trees using UAV acquired photogrammetric point clouds and object-based image analysis. Biosyst. Eng. 176, 172–184. https://doi.org/10.1016/j.biosystemseng.2018.10.018.
Trentacoste, E.R., Connor, D.J., Gomez-del-Campo, M., 2015. Effect of row spacing on vegetative structure, fruit characteristics and oil productivity of N-S and E-W oriented olive hedgerows. Sci. Hortic. 193, 240–248. https://doi.org/10.1016/j.scienta.2015.07.013.
Virlet, N., Gomez-Candon, D., Lebourgeois, V., Martinez, S., Jolivot, A., Lauri, P.E., Costes, E., Labbe, S., Regnard, J.L., 2016. Contribution of high-resolution remotely sensed thermal-infrared imagery to high-throughput field phenotyping of an apple progeny submitted to water constraints. Acta Horticulture 1127, 243–250. https://doi.org/10.17660/ActaHortic.2016.1127.38.
Zeinanloo, A., Shahsavari, A., Mohammadi, A., Naghavi, M.R., 2009. Variance component and heritability of some fruit characters in olive (Olea europaea L.). Sci. Hortic. 123, 68–72. https://doi.org/10.1016/j.scienta.2009.07.024.